Rahim *et al.*
Egypt J Neurol Psychiatry Neurosurg (2023) 59:60
https://doi.org/10.1186/s41983-023-00649-z

The Egyptian Journal of Neurology, Psychiatry and Neurosurgery

REVIEW

Open Access

Metabolite changes in the posterior cingulate cortex could be a signature for early detection of Alzheimer's disease: a systematic review and meta-analysis study based on ^{1}H-NMR

Fakher Rahim[1], Mohammad Khalafi[2], Mohammad Davoodi[3] and Kiarash Shirbandi[4*]

Abstract

Background Posterior cingulate cortex (PCC) is a paralimbic cortical structure with a fundamental role in integrative functions of the default mode network (DMN). PCC activation and deactivation of interconnected structures within the medial temporal lobe is essential in memory recall.

Aim Assessing the metabolomics content changes in PCC of the patients with Alzheimer's disease (AD) compared to healthy controls (HC) to find a new method for early AD detection was the primary goal of this study.

Methods We performed a comprehensive search through eight international indexing databases. Searches were done using the medical subject headings (Mesh) keywords. Outcome measures included Population (HC/AD), Age (y), Gender (Male/Female), MRI equipment, Tesla (T), MMSE (mean ± SD), absolute and ratio absolutes metabolites in the PCC. All meta-analyses were performed using STATA V.14 tools to provide pooled figures.

Results Studies published from 1980 to 2019 using the ^{1}H-NMR technique of 3,067 screened studies, 18 studies comprising 1647 people (658 males and 941 females, 921 HC and 678 AD cases) were included. The results revealed a significant increase in ml content and a substantial decrease in NAA, Glu, and Glx levels of the PCC in AD patients compared to HC.

Conclusions Our meta-analysis showed that microstructural disruptions in the PCC could be used as a marker for early AD detection. Although NAA, ml, Glu, and (NAA, Cho, and ml)/Cr biomarkers are substantial metabolites for diagnosis and are most sensitive for diagnosis.

Trial registration PROSPERO Registration: CRD42018099325.

Keywords Proton nuclear magnetic resonance (^{1}H-NMR), Neurodegenerative diseases, Alzheimer's disease (AD), Metabolomics, Biomarker, Gyrus cinguli, Posterior cingulate cortex (PCC)

*Correspondence:
Kiarash Shirbandi
shirbandi.k@gmail.com
Full list of author information is available at the end of the article

Introduction

The most prevalent cause of dementia is Alzheimer's disease (AD), characterized by regional brain atrophy, memory deficits, and deterioration of executive functions [1, 2]. AD causes memory and executive function problems, affects other cognitive domains, and causes neuropsychiatric symptoms. AD is a multifactorial disease, however, the etiopathogenesis not being fully understood. Amyloid precursor protein metabolism, phosphorylated tau aggregation, impaired kynurenic acid pathway, and mitochondrial dysfunction are identified as culprits in disease pathology. Lower nicotinamide adenine dinucleotide (NAD+) secondary to impaired tryptophan-kynurenine metabolic system causes aerobic respiration dysfunction which leads to anaerobic respiration and energy loss in AD [3–7]. With the increase in life expectancy, it is predicted that in 2050, more than 106 million people will be diagnosed with AD worldwide, while in 2006, the number of patients was equal to 26 million [8, 9]. Amyloid and tau pathologies, which have different structural abnormalities, are two distinct pathologies that manifest at various stages of the disease's progression. It has been proposed that when the amyloid and tau diseases overlap, the sickness may turn into a distinct illness [10–12]. Prior to that, specific characteristics may have been linked to the development of just plaques in specific brain regions [13].

The posterior cingulate cortex (PCC) is a paralimbic cortical structure located in the core hub of the default mode network (DMN), with a fundamental role in the integrative functions of the DMN, including memory processing and encoding [14]. During episodic memory recall activity, there is the deactivation of the PCC and hippocampal activation. PCC interactions with the hippocampal gyrus of the medial temporal lobe (MTL) network and prefrontal cortical regions are essential for their role in cognitive function. Prominent Aβ deposition and hypo-metabolism in PCC, despite a low degree of atrophy, support the idea of the vital role of PCC dysfunction in connectivity disruption and memory loss associated with AD [15–17].

The measurement of the metabolome is related to a novel field of research with increasing importance called metabolomics [18]. This field can aid us by providing a comprehensive diagnosis of neurodegenerative disorders by characterizing absolute metabolites in a specific sample. Metabolomics is more sensitive to environmental and physical factors than genomics and proteomics [19]. Hence, to evaluate the metabolomics content changes in PCC, it can be helpful to compare AD patients and healthy individuals by the metabolome content in PCC [20].

Early diagnosis of AD has been one of the hot-spot research focus, fluid biomarkers, as well as neuroimaging techniques, have been utilized to elucidate the pathophysiology of early AD [21, 22]. The loss of functional integrity of the frontal and hippocampal-based memory systems in individuals can be utilized as a measure of neurodegenerative processes in individuals with a high risk of dementia or with a diagnosis of AD: evidence from recent studies provided an overview of the anatomical–functional interplay between the prefrontal cortex and heart-related dynamics in human emotional conditioning (learning). It proposed a theoretical model to conceptualize these psychophysiological processes, the neurovisceral integration model of fear (NVI-f), that can be impaired in neurodegenerative disorders [23, 24]. Nuclear magnetic resonance (NMR), positron-emission tomography (PET), and mass spectrometry (MS) with conventional techniques have raised hope of achieving this goal [5].

Proton nuclear magnetic resonance (^{1}H-NMR), also called NMR spectroscopy, helps us measure quantitatively microstructural disruptions. Different electron shielding around the metabolites is the discriminative factor in assessing the signals of each metabolite in a strong magnetic field [25]. NMR spectroscopy-based metabolomics is a non-invasive method that does not require complex manipulation protocols of samples. Although for a precise and comparable measure of brain metabolites, MR spectroscopy needs some (and sometimes many) manipulations of protocols post-processing and is subjected to many artifacts. So, it is not a simple technique. The standardizing methods are the main limitation of applying spectroscopy on a large scale and comparing it in different centers [26, 27]. Therefore, this study aimed to look at the similarities and discrepancies of the studies, critically review the advantages and limitations of using NMR spectroscopy as a marker of AD, and investigate the metabolites changes in PCC as one of the signature AD regions in AD patients compared to HC.

Methods

The systematic review and meta-analysis protocol was registered in the PROSPERO, a prospective international register of systematic reviews under record number *CRD42018099325*. This study was done with standard guidelines such as the Preferred Reporting Items for Systematic Reviews and Meta-Analyses (PRISMA) guidelines [28] and the Meta-analysis of Observational Studies in Epidemiology (MOOSE) [29].

Study criteria

The cohort, cross-sectional, and case–control design studies were included and evaluated metabolomics

changes in PCC patients with AD through the ^{1}H-NMR technique. Patients will be recruited if they are above 65 with the AD diagnosis by altered biomarkers (CSF or PET-scan) and clinical symptoms. Outcome measures included Population (HC/AD), Age (y), Gender (Male/Female), MRI equipment, Tesla (T), MMSE (mean ± SD), absolute and ratio absolutes metabolites in the PCC. HC group were all age and sex-matched with the AD patients and had no history of neuropsychological disorders.

Search methods

ISI Web of Science, Cochrane Library, PROSPERO, PubMed, Scopus, CINAHL, Science Direct from inception, EMBASE, and any of the included research reference lists.

The search was started in 2000 until May 2019. Searches were done using the medical subject headings (Mesh) keywords ("*^{1}H-NMR*" OR "*MRS*" OR "*Magnetic Resonance Spectroscopy*") AND ("*Alzheimer disease*" OR "*Dementia*") AND ("*Metabolite*" OR "*Metabolomics*"). Any meta-analysis, review studies (narrative or systematic), case series or case reports, commentaries, and letters to the editor were excluded. Studies fulfilling the above criteria, with a cohort, cross-sectional, or case–control design, and full-text information were available and considered in the meta-analysis.

In our data collection, studies were included whether they were about brain ^{1}H-NMR, examined individuals with AD, comprised healthy control groups, and compared absolute metabolites in the PCC region. The importance of knowledge was independently derived from experiments by two scholars (K.SH. and F.R.) If applicable, we have contacted the writers of the qualifying papers for missing details.

Quality assessment

Quality assessment was assessed according to standardized tools for grading cohort studies (Newcastle Ottawa-Scale [30]). Newcastle Ottawa-Scale is a tool to assess risk of bias and quality used in a systematic review study with included non-random studies.

Publication bias

The visual inspection of the funnel plots and the Egger test for each group and each metabolite were used to observe the propensity for publishing bias [31]. A significance level of $P<0.10$ defined significant publishing bias based on the Cochrane handbook for systematic reviews [31].

Sensitivity analysis

Sensitivity analysis based on study quality (risk of bias) to investigate possible sources of heterogeneity. The primary decision nodes concluded methodological consistency, sample size, and the impact of missed data. The researchers replicated the meta-analysis, and low-quality findings were omitted. The outcome was contrasted and debated based on the extracted conclusions from other researchers.

Statistical analysis

All meta-analyses were carried out using STATA V.14 tools to provide pooled figures, with a corresponding 95 percent confidence interval (CI) and plots for studies disclosing absolute metabolite and metabolite ratio in the PCC. The mean estimates of each sample were pooled using a model of random effects for meta-analysis [32]. The I^2 figures and the Chi-square test have been used to test heterogeneity. It was considered that $I^2>50$ percent or $P<0.05$ demonstrated substantial heterogeneity. In addition, to determine publishing bias, the funnel plot and the Egger regression test were added.

Results

Study selection

A comprehensive search of the literature conducted a total of 3067 relevant studies. A total of 764 were excluded after duplicates. Title—the abstract screening was excluded, and several 2276 studies and 27 full texts were selected (Fig. 1). At last, 18 original articles with cross-sectional or case–control design, comprising 1647 cases, [658 (40%) males and 941 (60%) females] were selected. Healthy controls (HC) 921 (55.9%) and AD 678 (44.1%) were included in the meta-analysis [33–50]. Nine studies were excluded after full-text screening (Additional file 1: Table S1) [51–59]. The mean age of the AD and HC participants was 73.33 ± 4.22 and 69.73 ± 7.15, respectively, and the Mini-Mental State Examination (MMSE) of the AD and HC were 19.45 ± 2.63 and 28.36 ± 1.27, respectively. Outlines of the search method and the number of studies excluded during each phase of the search are provided in Fig. 1. The table gives a detailed overview of the study population of each of the 18 reviewed studies (Table 1).

A. Metabolite concentration

Metabolite concentrations were reported in 8 studies. *N*-Acetyl aspartate (NAA), creatine (Cr), choline (Cho), myo-inositol (mI), glutamine (Glu), and glutamate + glutamine (GLx) concentrations were extracted as the target variables (Table 1). On the one hand, results displayed a significant increase in mI content of the PCC in AD group compared to controls (0.32 [95% CI 0.19, 0.46]) (Table 2) (Additional file 1: Figs. S1–S5); on the other hand, there was significant decrease in NAA, Glu, and Glx levels of the PCC in AD participants compared to

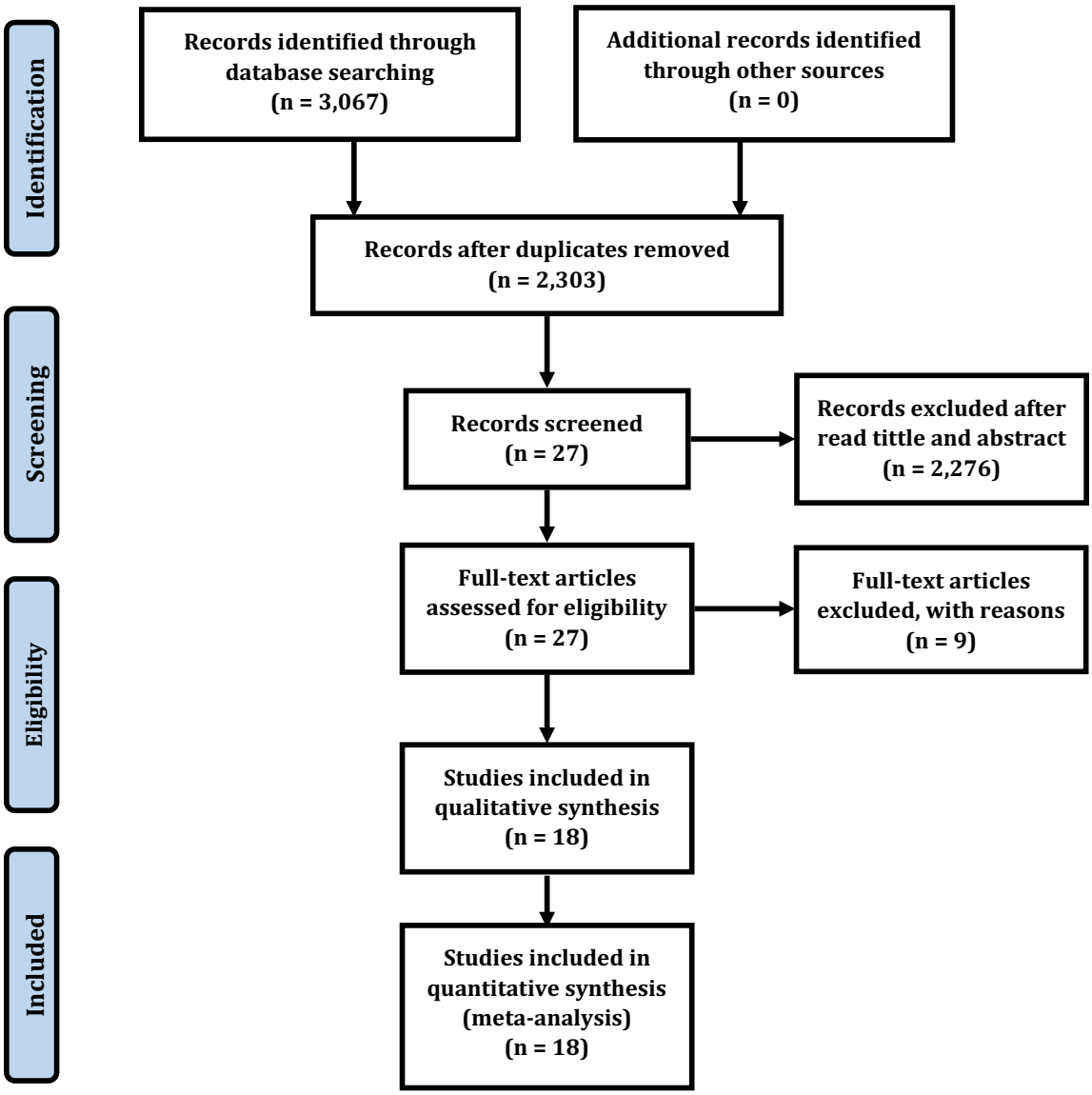

Fig. 1 Study flow diagram showing how to extract articles

HC, (mean difference = 0.91 [95% CI −1.05, −0.77], 0.75 [95% CI −1.00, −0.50], and 0.67 [95% CI −1.13, −0.20], respectively) (Table 2) (Additional file 1: Figs. S6 and S7). No significant difference between AD and HC groups was observed in the concentration of Cr and Cho (Figs. 2, 3, 4).

B. Metabolite ratio

Metabolite ratios reported in 18 studies, NAA/Cr, NAA/mI, Cho/Cr, mI/Cr, scyllo-inositol (sI)/Cr, mI/NAA, Glu/Cr, mI/Cho were extracted (Table 1). The results revealed a significant decrease in NAA/Cr ratio (mean difference = 0.15 [95% CI −0.20, −0.09]) (Fig. 5), however, the results for Cho/Cr (0.05 [95% CI 0.03, 0.06]) (Fig. 5) and mI/Cr ratio (0.10 [95% CI 0.08, 0.13]) (Fig. 6) were associated with significant increase in the AD group compared to controls (Table 2; Additional file 1: Figs. S8–S13). No significant differences were found in the PCC mI/NAA ratio between the AD and HC groups (Fig. 6). Due to insufficient studies, we could not conduct a meta-analysis for NAA/mI, SI/Cr, Glu/Cr, and mI/Cho ratios (Fig. 7).

Table 1 Characteristic of included studies on various metabolites between patient with Alzheimer's disease (AD) and healthy controls (HC)

Study ID	Population (HC/AD)	Age y, mean ± SD (range)		Male/female	Tesla (T)	TR/TE (ms)	Pulse	Voxel size	Disease phase	MMSE (mean ± SD)		Metabolites	
		HC	AD							HC	AD	Ratio	Absolute
Griffith et al. 2007, USA	34 (19/15)	67.47 ± 5.74	69.42 ± 6.62	11/23	3.0	2000/32	–	8 ml	Mild	29.58 ± 0.84	24.71 ± 2.95	NAA/Cr, ml/Cr, sI/Cr	–
Kantarci et al. 2007, USA	148 (88/60)	79.1 ± 7.2	78.0 ± 8.5	68/80	1.5	2000/30	PRESS	8 ml	Mild	29.0 ± 1.0	23.0 ± 2.0	NAA/Cr, Cho/Cr, ml/Cr	–
Ding et al. 2008, China	40 (20/20)	71.9 ± 6.8	67.4 ± 8.9	13/27	1.5	1500/35	PRESS	8 ml	Moderate	28.3 ± 1.0	19.5 ± 2.9	NAA/Cr, Cho/Cr, ml/Cr	–
Wang et al. 2009, China	32 (16/16)	71.13 ± 11.13	72.13 ± 8.04	8/24	3.0	1700/30	PRESS	–	–	–	–	NAA/Cr, Cho/Cr, ml/Cr, ml/NAA	–
Watanabe et al. 2010, Japan	122 (52/70)	69.4 ± 6.1	72.1 ± 7.6	38/84	1.5	2000/30	PRESS	–	Mild	29.0 ± 1.4	20.8 ± 3.6	–	NAA, Cr, Cho, ml
Fayed et al. 2011, Spain	56 (26/30)	74.2 ± 6.9	69.96 ± 17.29	20/36	1.5	2000/35	–	8 ml	–	–	–	NAA/Cr, Cho/Cr, ml/Cr, Glu/Cr, GLx/Cr	NAA, Cho, ml, Glu, GLx
De Souza et al. 2011, Brazil	58 (33/25)	72.72 ± 7.08	77.96 ± 7.72	21/37	1.5	1500/31	PRESS	8 ml	Mild	27.7 ± 2.09	20.45 ± 4.59	NAA/Cr, ml/Cr, Cho/Cr, ml/NAA	–
Zimny et al. 2011, Poland	45 (15/30)	69.0 ± 7.9	71.5 ± 11.7	16/29	1.5	1500/35	PRESS	8 ml	Moderate	29.8 ± 0.4	18.0 ± 5.4	NAA/Cr, ml/Cr, Cho/Cr ml/NAA ml/Cho	–
Lim et al. 2012, Republic of Korea	45 (22/23)	68.1 ± 8.2	74.5 ± 8.7	10/35	3.0	2000/144	PRESS	1.5 × 1.5 × 2 cm	Moderate	25.8 ± 4.5	18.5 ± 5.6	NAA/Cr	–
Lim et al. 2012, Republic of Korea	59 (23/36)	68.1 ± 8.1	74.3 ± 9.6	14/35	3.0	2000/9.147	–	8 ml	Moderate	27.0 ± 4.4	18.8 ± 5.3	NAA/Cr, ml/Cr	–
Shiino et al. 2012, Japan	144 (45/99)	69.6 ± 6.1	72.2 ± 8.4	92/52	1.5	2000/30	PRESS	–	Moderate	29.1 ± 1.2	19.7 ± 3.4	NAA/Cr, Cho/Cr, ml/Cr, ml/NAA	NAA, Cr, Cho, ml, GLx
Wang et al. 2012, China	103 (56/47)	71.4 ± 9.7	70.9 ± 9.2	41/62	3.0	1500/35	PRESS	8 ml	Moderate	26.5 ± 3.5	13.8 ± 5.4	NAA/Cr, ml/Cr, Cho/Cr, NAA/ml	–
Watanabe et al. 2012, Japan	121 (54/67)	69.5 ± 6.2	72.3 ± 7.5	38/83	1.5	2000/30	PRESS	–	Mild	29.1 ± 1.4	20.6 ± 3.5	–	NAA, ml

Table 1 (continued)

Study ID	Population (HC/AD)	Age y, mean ± SD (range)		Male/female	Tesla (T)	TR/TE (ms)	Pulse	Voxel size	Disease phase	MMSE (mean ± SD)		Metabolites	
		HC	AD							HC	AD	Ratio	Absolute
Fayed et al. 2014, Spain	229 (193/36)	45.1	80.4	85/144	1.5	2000/35	PRESS	8 ml	–	–	–	NAA/Cr, ml/Cr, Cho/Cr, Glx/Cr	NAA, Glu, Cho, ml, GLx
Graff-Radford et al. 2014, USA	183 (148/35)	77 ± 6	79 ± 11	97/86	1.5	2000/30	–	8 ml	–	–	–	NAA/Cr, ml/Cr, Cho/Cr	–
Zou et al. 2014, China	40 (20/20)	64.94 ± 7.93	64.84 ± 8.82	17/23	3	1500/35	PRESS	20 × 20 × 20 mm	Moderate	27.35 ± 1.01	16.21 ± 4.01	NAA/Cr, Cho/Cr, ml/Cr	–
Jahng et al. 2016, Republic of Korea	71 (47/24)	69.67 ± 6.58	74.83 ± 8.03	29/42	3	2000/35	PRESS	1 × 1 × 1 mm^3	Moderate	29.74 ± 0.55	18.96 ± 5.09	–	NAA, Cr, mIns, Glx, Glu
Su et al. 2016, UK	69 (34/35)	76.8 ± 5.2	78.3 ± 5.8	40/29	3	3450/35	–	–	Moderate	29.1 ± 1.0	19.3 ± 4.3	Cho/Cr, NAA/Cr, ml/Cr, Glx/Cr	–

NAA N-acetyl aspartate, *Cr* creatine, *Glx* glutamate + glutamine, *Cho* choline, *ml* myo-inositol, *Glu* glutamine, *sI* scyllo-inositol

Table 2 Summary of outcome of subgroup analysis of various metabolites between patient with Alzheimer's disease (AD) and healthy controls (HC)

Metabolites	No. of studies	No. of AD	N of HC	Heterogeneity test		I^2 (%)	Model	Effect estimate (95% CI)	Test(s) of $P=0$	
				Chi^2	*P*-value				*Z*	*P*-value
Concentration										
NAA	6	326	417	2.15	0.83	0	Fixed	−0.91 [−1.05, −0.77]	12.47	**< 0.00001**
Cr	2	169	97	5.36	0.02	81	Random	−0.33 [−0.81, 0.15]	1.33	0.18
Cho	4	235	316	0.64	0.84	0	Fixed	0.03 [−0.01, 0.07]	1.67	0.89
ml	5	302	370	1.10	0.89	0	Fixed	0.32 [0.19, 0.46]	4.65	**< 0.00001**
Glu	3	90	266	0.37	0.83	0	Fixed	−0.75 [−1.00, −0.50]	5.87	**< 0.00001**
GLx	4	189	311	7.66	0.05	61	Random	−0.67 [−1.13, −0.20]	2.80	**0.005**
Ratio										
NAA/Cr	14	491	735	174.71	< 0.00001	93	Random	−0.15 [−0.20, −0.09]	5.30	**< 0.00001**
Cho/Cr	13	464	739	54.16	< 0.00001	78	Random	0.05 [0.03, 0.06]	5.38	**< 0.00001**
ml/Cr	16	632	1005	104.68	< 0.00001	86	Random	0.10 [0.08, 0.13]	8.66	**< 0.00001**
ml/NAA	7	266	367	162.48	< 0.00001	96	Random	0.17 [0.04, 0.30]	2.51	0.01
NAA/ml	1	47	56	–	–	–	–	–	–	–
sl/Cr	1	15	19	–	–	–	–	–	–	–
Glu/Cr	1	30	26	–	–	–	–	–	–	–
ml/Cho	1	30	15	–	–	–	–	–	–	–

Bold values indicate a signidicante value relationship between AD and healthy controls

N number

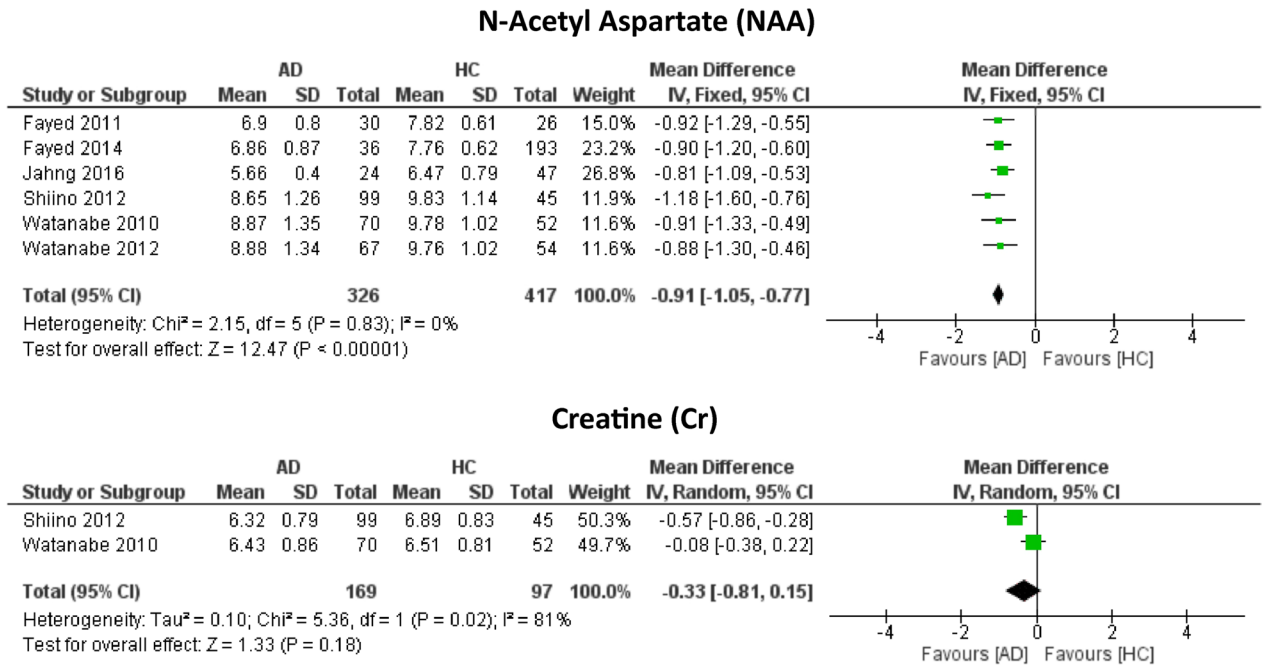

Fig. 2 Compared to healthy controls, forest plots of comparison *N*-acetyl aspartate (NAA) and creatine (Cr) in AD patients. Data type: continuous; effect size: Hedges' *g*; effect model: fixed and random model; CI: confidence interval

Discussion

According to this meta-analysis, in PCC absolutes, substantial variations were observed between early detection AD patients and HC of the *NAA*, *mI*, *Glu*, and *Glx* and metabolite ratios, including *NAA/Cr*, *Cho/Cr*, and *mI/Cr*. There was no significant difference in *Cr* and *Cho* levels and *mI/NAA* ratio in early detection AD compared with HC groups. The hippocampus, crucial for declarative

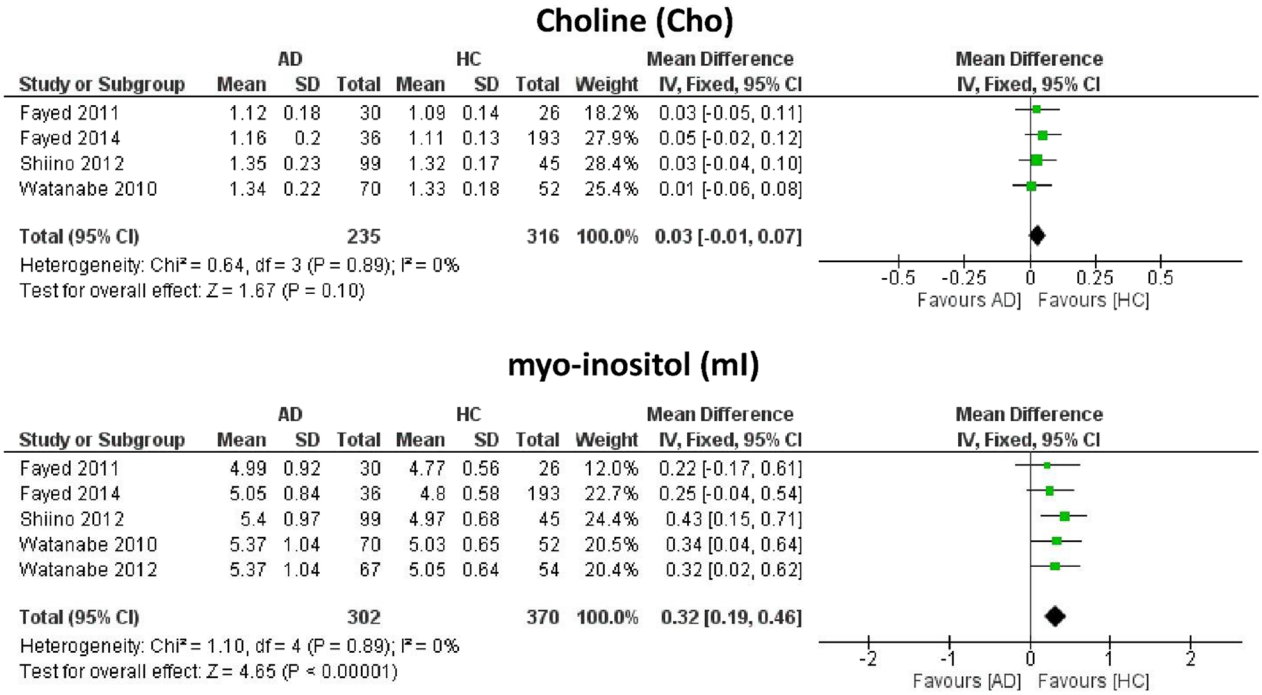

Fig. 3 Forest plots of comparison choline (Cho) and myo-inositol (ml) in AD patients compared to healthy controls. Data type: continuous; effect size: Hedges' *g*; effect model: fixed model; CI: confidence interval

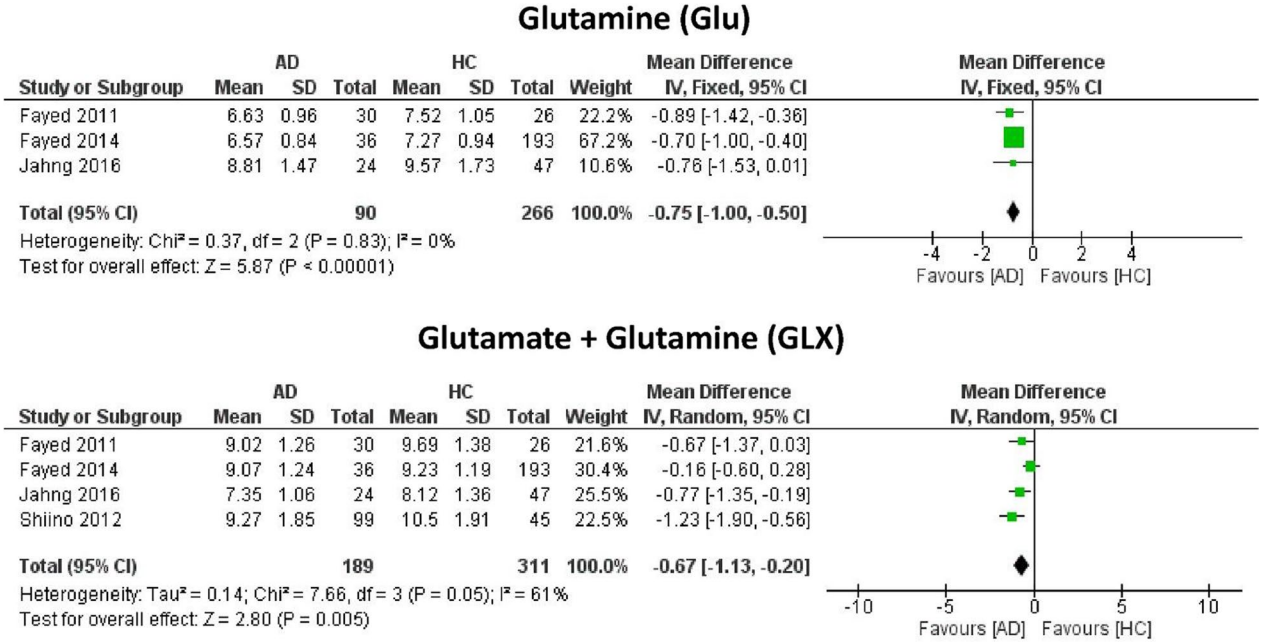

Fig. 4 Compared to healthy controls, forest plots of comparison glutamine (Glu) and glutamate + glutamine (GLX) in AD patients. Data type: continuous; effect size: Hedges' *g*; effect model: fixed and random model; CI: confidence interval

memory, serves as the physical hallmark of AD [60]. Potential indicators for predicting the transition from MCI to AD include hippocampal shrinkage and its rate of atrophy [61]. It has also been shown that functional and structural networks connected to the hippocampus have decreased integrity [62]. Although different studies use

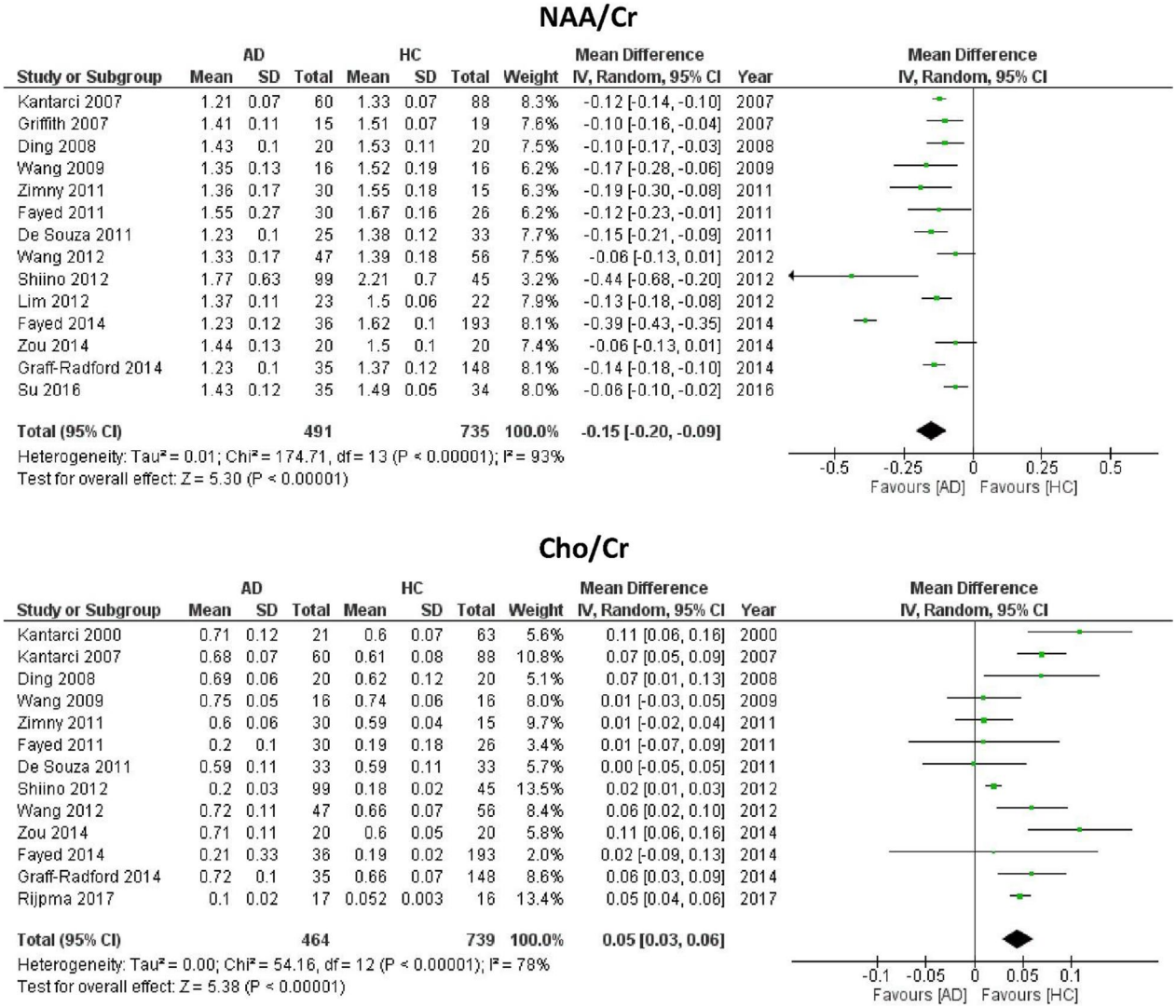

Fig. 5 Compared to healthy controls, forest plots of NAA/Cr and Cho/Cr in AD patients. Data type: continuous; effect size: Hedges' *g*; effect model: random model; CI: confidence interval

different network mapping techniques, the geographical distribution of the discovered synchronized degeneration networks (SDNs) with hippocampal epicenters is remarkably consistent with earlier research [63]. Numerous AD histological and neuroimaging discoveries have suggested that the hippocampus and surrounding areas, generally known as the medial temporal lobe, have close relationships [64, 65]. According to a large body of research, the hippocampus and prefrontal cortex connect via oscillatory synchrony, reflecting bidirectional information flow, and may play a significant role in memory and learning outside of the limbic system [66]. These regional and network-level discoveries highlight the significance of the hippocampus and the related functionally and structurally connected regions in the pathophysiology of AD [67].

NAA is synthesized in the mitochondria of the brain cell and is considered a marker of neuronal integrity, visibility, density, functional mitochondria, and capacity in brain tissues [68]. The remarkable decline in the absolute metabolite in AD patients will represent neuronal loss and mitochondrial function [69]. Therefore, a significant decrease in NAA levels of the PCC would directly reflect early detection of AD pathology in this region. ^{1}H-NMR studies have also shown a widespread reduction in *NAA/Cr* ratio in AD patients and its association with extensive neuronal dysfunction and loss [54]. NAA/cr is thus one of the sensitive markers for AD, in line with our

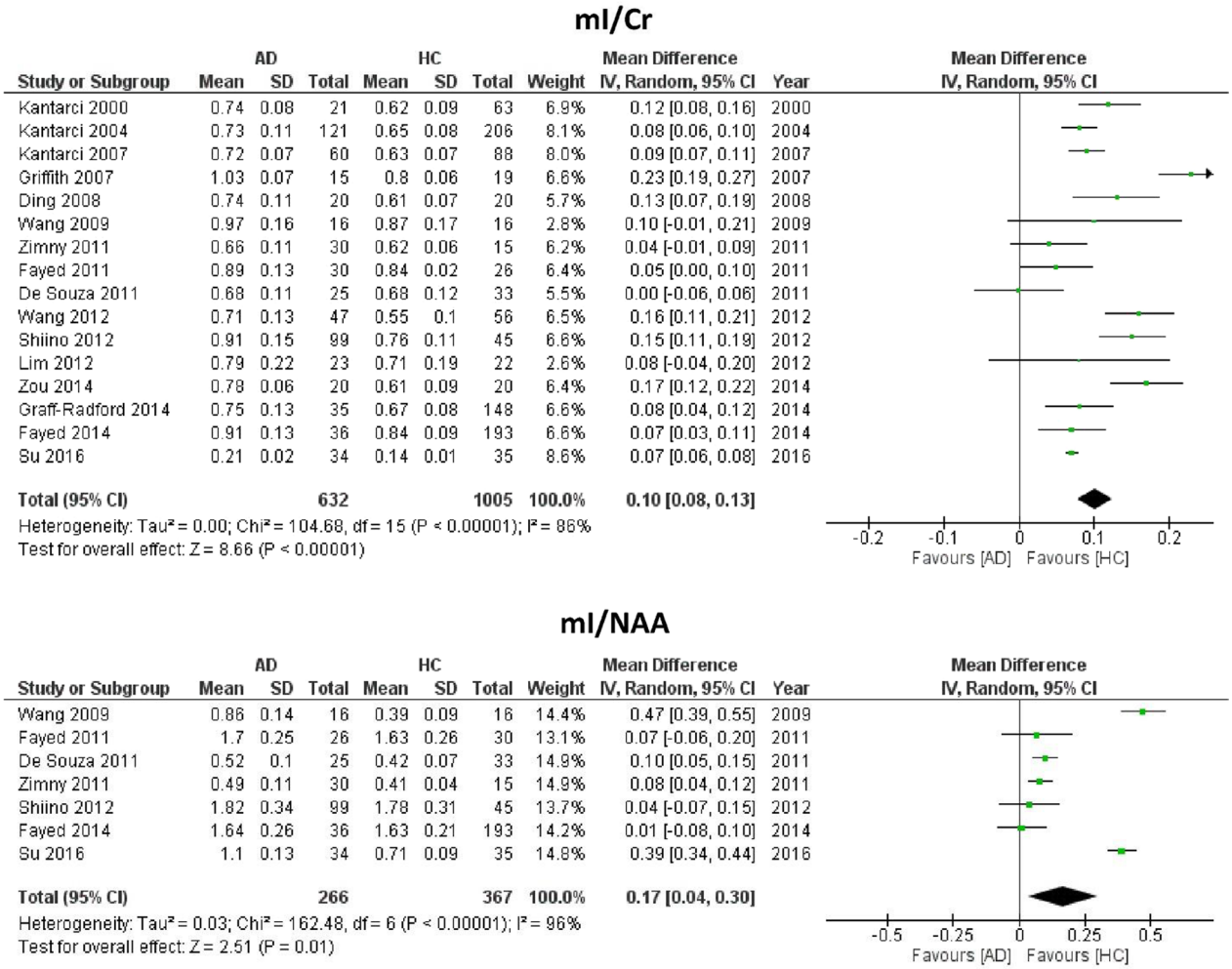

Fig. 6 Forest plots of mI/Cr and mI/NAA in AD patients compared to healthy controls. Data type: continuous; effect size: Hedges' *g*; effect model: random model; CI: confidence interval

findings of decreased NAA/cr ratio in the PCC [54, 70, 71]. *Cho* is mainly present in myelin and cell membranes as Cho-bound membrane phospholipids [72]. Free Cho and acetylcholine absolute cytosol are hardly detectable through ^{1}H-NMR due to their low absolute in brain tissues [73]. An elevated level of Cho detected by ^{1}H-NMR is attributed to the catabolism of phosphatidylcholine in the neuron membrane to provide free choline molecules in the cytosol, increasing it in absolute [51, 73]. Similarly, disinhibited regulation of choline acetyltransferase due to neuronal dysfunction can lead to high absolute Cho, justifying the high *Cho/Cr* level in early detection AD patients that can be interpreted into changes in membrane metabolism and neuronal membrane disruption. γ-Secretase is a complex of transmembrane proteases which consists of the PEN2, PSEN, NCSTN, and APH-1 monomers, and The breakdown of the amyloid precursor protein into insoluble amyloid β-peptides (Aβ) is responsible for and is regulated by SLC2A13, which was a target in AD for Aβ reduction therapy [74, 75]. *SLC2A13 also encodes the (H+) myo-inositol* co-transporter and is essential in the metabolic regulation of glial cells. Increased mI in PCC could reflect SLC2A13 downregulation, γ-secretase overactivation, and increased Aβ production deposition in PCC in early AD [75].

Last but not least, glutamate is the primary central nervous system (CNS) excitatory transmitter, which plays a significant part in thought, memory, and plasticity [76]. These metabolites are synthesized from *glutamine* by *glutaminase* in neurons [77]. The *N*-methyl-D-aspartate receptor (NMDAR) is usually the most calcium-permeable (Ca2+) receptor and type of *glutamate* receptor [78]. The receptor can interact between beta oligomers and *glutamine*, *glutamate,* or *glutamine*+*glutamate (Glx)* metabolites.

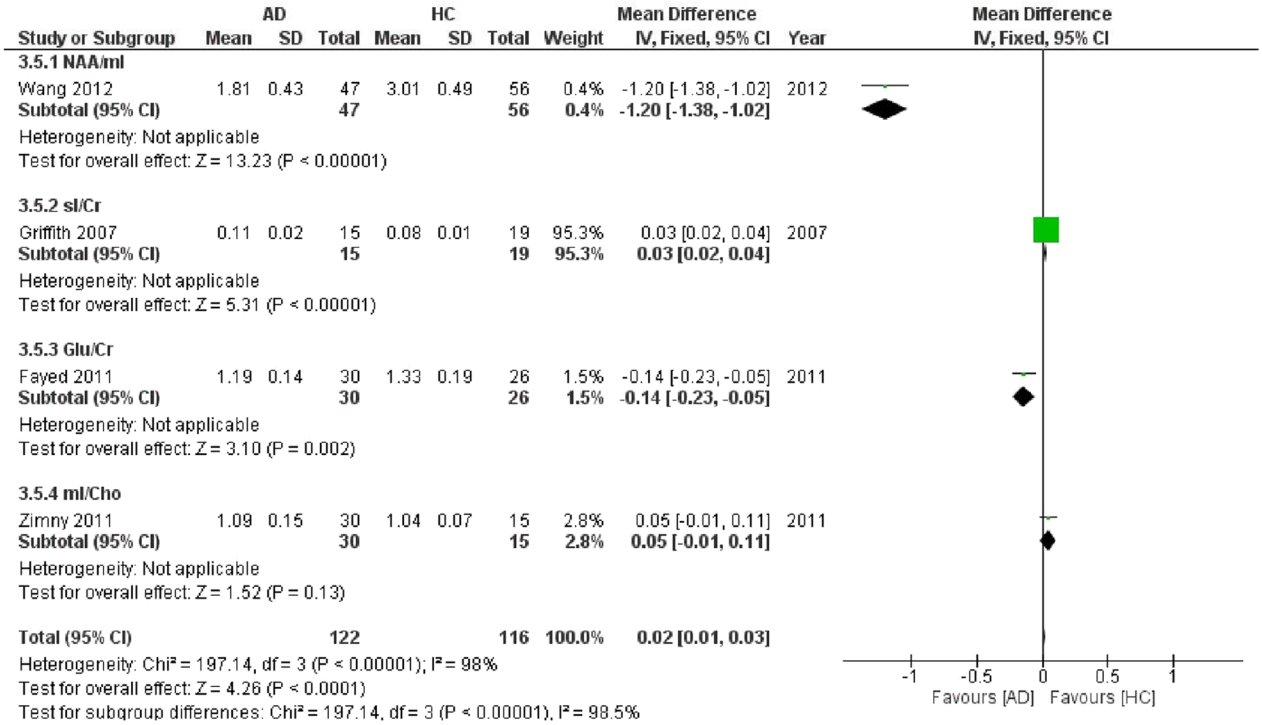

Fig. 7 Forest plot of comparison single metabolites in AD patients compared to healthy controls. Data type: continuous; effect size: Hedges' *g*; effect model: random model; CI: confidence interval

Limitations and future directions

Sample sizes were relatively small, and randomized clinical trial (RCT) studies were not included, requiring more significant diagnostic accuracy. The real added value will come from new studies where metabolomics technologies are added to evaluate changes in metabolism in the brain and peripherally spectroscopy and the interconnections between both. Therefore, what has been done so far is limited insights into metabolism using a small number of markers that authors are reviewing. The combination of imaging and genomics has proved to be a powerful pair, but a critical question may come to mind: could imaging be equally valuable for metabolomics? Some researchers think it might, particularly with the adoption of ^{1}H-NMR. Our meta-analysis showed that metabolite changes in the posterior cingulate cortex could be used as a marker for the early detection of Alzheimer's disease. NAA and ml, and Cho/Cr ratio biomarkers seem to be substantial metabolites for early detection of AD, which can be of interest to researchers. It is recommended to design studies similar to the studies analyzed here but with a more significant number of participants by age group, as well as taking into account the years that have passed since the early diagnosis.

Conclusions

Our meta-analysis showed that microstructural disruptions in the PCC could be used as a marker for early AD detection. Although NAA, mI, Glu, and (NAA, Cho, and mI)/Cr biomarkers are substantial metabolites for diagnosis and are most sensitive for diagnosis. The critical biomarker can be of interest to researchers. Two susceptible areas involved in the pathophysiology of AD early on are the PCC and the hippocampus. Notably, the PCC-epicentered network predicts AD development, including brain atrophy and cognitive impairment, but not the hippocampus-epicentered network. Our findings lend credence to the network degeneration concept of AD and imply that PCC could be employed as possible disease-progression markers. The findings also shed light on the mechanisms behind network disease in AD.

Abbreviations

AD	Alzheimer's disease
ml	Myo-inositol
PCC	Posterior cingulate cortex
HC	Healthy control
NAA	*N*-Acetyl aspartate
Glu	Glutamine
Glx	Glutamate + glutamine
Cr	Creatine
Cho	Choline
DMN	Default mode network

MTL	Medial temporal lobe
CSF	Cerebrospinal fluid
NMR	Nuclear magnetic resonance
PET	Positron-emission tomography
MS	Mass spectrometry
^{1}H-NMR	Proton nuclear magnetic resonance
PRISMA	Reporting Items for Systematic Reviews and Meta-Analyses
MOOSE	Meta-analysis of Observational Studies in Epidemiology
MMSE	Mini-Mental State Examination
Aβ	Amyloid β-peptides
NMDAR	*N*-Methyl-D-aspartate receptor

Supplementary Information

The online version contains supplementary material available at https://doi.org/10.1186/s41983-023-00649-z.

Additional file 1. Search strategy and selection criteria. Metabolomics-biomarkers of Alzheimer. **Table S1.** Study exclusion. **Figure S1.** Forest plot of comparison N-Acetyl Aspartate. **Figure S2.** Funnel plot of comparison N-Acetyl Aspartate. **Figure S3.** Forest plot of comparison Creatine. **Figure S4.** Forest plot ofcomparison Choline. **Figure S5.** Forest plot of comparisonmyo-inositol. **Figure S6.** Forest plot of comparison glutamine. **Figure S7.** Forest plot of comparison glutamate + glutamine. **Figure S8.** Funnel and Forest plot of comparison NAA/Cr. **Figure S9.** Funnelplot of comparison NAA/Cr. **Figure S10.** Funnel and Forest plot of comparison-Cho/Cr. **Figure S11.** Funnel and Forest plot of comparison mI/Cr. **Figure S12.** Funnel and forest plot of comparison mI/NAA. **Figure S13.** Single metabolites.

Acknowledgements
Not applicable.

Author contributions
KSH, MD: designed data collection tools, monitored data collection, wrote the statistical analysis plan, cleaned, and analyzed the data, and drafted and revised the paper. KSH: wrote the statistical analysis plan, cleaned, and analyzed the data. MK, FR: implemented the study, analyzed the data, drafted, and revised the paper. All authors read and approved the final manuscript.

Funding
Not applicable.

Availability of data and materials
Not applicable.

Declarations

Ethics approval and consent to participate
Not applicable.

Consent for publication
Not applicable.

Competing interests
The authors declare that they have no competing interests.

Author details
[1]Department of Anesthesia, Cihan University - Sulaimaniya, Sulaymaniyah, Kurdistan Region, Iraq. [2]School of Medicine, Tabriz University of Medical Sciences, Tabriz, Iran. [3]Department of Radiology, Shariati Hospital, Tehran University of Medical Sciences, Tehran, Iran. [4]Research Center for Molecular and Cellular Imaging, Tehran University of Medical Sciences, Tehran, Iran.

Received: 9 August 2021 Accepted: 23 March 2023
Published online: 05 May 2023

References

1. Pimplikar SW, et al. Amyloid-independent mechanisms in Alzheimer's disease pathogenesis. J Neurosci. 2010;30(45):14946–54.
2. Bateman RJ, et al. Clinical and biomarker changes in dominantly inherited Alzheimer's disease. N Engl J Med. 2012;367(9):795–804.
3. Selkoe DJ, Hardy J. The amyloid hypothesis of Alzheimer's disease at 25 years. EMBO Mol Med. 2016;8(6):595–608.
4. Fazio S, et al. The fundamentals of person-centered care for individuals with dementia. Gerontologist. 2018;58(suppl_1):S10–9.
5. Scheltens P, et al. Alzheimer's disease. Lancet. 2016;388(10043):505–17.
6. Martos D, et al. Memory enhancement with kynurenic acid and its mechanisms in neurotransmission. Biomedicines. 2022;10(4):849.
7. Tanaka M, et al. Mitochondrial impairment: a common motif in neuropsychiatric presentation? The link to the tryptophan–kynurenine metabolic system. Cells. 2022;11(16):2607.
8. Brookmeyer R, et al. Forecasting the global burden of Alzheimer's disease. Alzheimers Dement. 2007;3(3):186–91.
9. Wilmoth JR, et al. Geographic differences in life expectancy at age 50 in the United States compared with other high-income countries. In: International differences in mortality at older ages: dimensions and sources. Washington, DC: National Academic Press; 2011. p. 333–66.
10. Tanaka M, Toldi J, Vécsei L. Exploring the etiological links behind neurodegenerative diseases: inflammatory cytokines and bioactive kynurenines. Int J Mol Sci. 2020;21(7):2431.
11. Di Gregorio F, et al. Accuracy of EEG biomarkers in the detection of clinical outcome in disorders of consciousness after severe acquired brain injury: preliminary results of a pilot study using a machine learning approach. Biomedicines. 2022;10(8):1897.
12. Hojjati SH, et al. Topographical overlapping of the amyloid-β and tau pathologies in the default mode network predicts Alzheimer's disease with higher specificity. J Alzheimers Dis. 2021;83(1):407–21.
13. Orso B, et al. The role of hub and spoke regions in theory of mind in early Alzheimer's disease and frontotemporal dementia. Biomedicines. 2022;10(3):544.
14. Hampson M, et al. Brain connectivity related to working memory performance. J Neurosci. 2006;26(51):13338–43.
15. Johnson KA, et al. Preclinical prediction of Alzheimer's disease using SPECT. Neurology. 1998;50(6):1563–71.
16. Greicius MD, et al. Default-mode network activity distinguishes Alzheimer's disease from healthy aging: evidence from functional MRI. Proc Natl Acad Sci USA. 2004;101(13):4637–42.
17. Buckner RL, et al. Molecular, structural, and functional characterization of Alzheimer's disease: evidence for a relationship between default activity, amyloid, and memory. J Neurosci. 2005;25(34):7709–17.
18. Bujak R, et al. Metabolomics for laboratory diagnostics. J Pharm Biomed Anal. 2015;113:108–20.
19. Rempel LA, Rohrer GA, Nonneman DJ. Genomics and metabolomics of post-weaning return to estrus. Mol Reprod Dev. 2017;84(9):987–93.
20. Raichle ME, et al. A default mode of brain function. Proc Natl Acad Sci USA. 2001;98(2):676–82.
21. Li Y, et al. Decreased CSF clearance and increased brain amyloid in Alzheimer's disease. Fluids Barriers CNS. 2022;19(1):1–9.
22. Zetterberg H, Blennow K. Moving fluid biomarkers for Alzheimer's disease from research tools to routine clinical diagnostics. Mol Neurodegener. 2021;16(1):10.
23. Battaglia S, Thayer JF. Functional interplay between central and autonomic nervous systems in human fear conditioning. Trends Neurosci. 2022;45(7):504–6.
24. Battaglia S, et al. Characterizing cardiac autonomic dynamics of fear learning in humans. Psychophysiology. 2022;59: e14122.
25. Bakalov V, et al. Metabolomics with nuclear magnetic resonance spectroscopy in a *Drosophila melanogaster* model of surviving sepsis. Metabolites. 2016;6(4):47.
26. Dona AC, et al. A guide to the identification of metabolites in NMR-based metabonomics/metabolomics experiments. Comput Struct Biotechnol J. 2016;14:135–53.
27. Kodani Y, et al. NMR-based metabolomics for simultaneously evaluating multiple determinants of primary beef quality in Japanese Black cattle. Sci Rep. 2017;7(1):1297.
28. Panic N, et al. Evaluation of the endorsement of the preferred reporting items for systematic reviews and meta-analysis (PRISMA) statement on

the quality of published systematic review and meta-analyses. PLoS ONE. 2013;8(12): e83138.
29. Stroup DF, et al. Meta-analysis of observational studies in epidemiology: a proposal for reporting. Meta-analysis of observational studies in epidemiology (MOOSE) group. JAMA. 2000;283(15):2008–12.
30. Wells G, et al. The Newcastle–Ottawa scale (NOS) for assessing the quality of nonrandomized studies in meta-analysis. 2011. http://www.ohri.ca/programs/clinical_epidemiology/oxford.asp. 2016.
31. Higgins JP, Green S. Cochrane handbook for systematic reviews of interventions, vol. 4. New York: Wiley; 2011.
32. Borenstein M, et al. A basic introduction to fixed-effect and random-effects models for meta-analysis. Res Synth Methods. 2010;1(2):97–111.
33. Griffith HR, et al. Elevated brain scyllo-inositol concentrations in patients with Alzheimer's disease. NMR Biomed. 2007;20(8):709–16.
34. Kantarci K, et al. Longitudinal 1H MRS changes in mild cognitive impairment and Alzheimer's disease. Neurobiol Aging. 2007;28(9):1330–9.
35. Ding B, et al. Diffusion tensor imaging correlates with proton magnetic resonance spectroscopy in posterior cingulate region of patients with Alzheimer's disease. Dement Geriatr Cogn Disord. 2008;25(3):218–25.
36. Wang Z, et al. Regional metabolic changes in the hippocampus and posterior cingulate area detected with 3-Tesla magnetic resonance spectroscopy in patients with mild cognitive impairment and Alzheimer disease. Acta Radiol. 2009;50(3):312–9.
37. Watanabe T, Shiino A, Akiguchi I. Absolute quantification in proton magnetic resonance spectroscopy is useful to differentiate amnesic mild cognitive impairment from Alzheimer's disease and healthy aging. Dement Geriatr Cogn Disord. 2010;30(1):71–7.
38. Fayed N, et al. Brain glutamate levels are decreased in Alzheimer's disease: a magnetic resonance spectroscopy study. Am J Alzheimers Dis Other Demen. 2011;26(6):450–6.
39. De Souza AS, et al. Contribution of 1H spectroscopy to a brief cognitive-functional test battery for the diagnosis of mild Alzheimer's disease. Dement Geriatr Cogn Disord. 2011;32(5):351–61.
40. Zimny A, et al. Multimodal imaging in diagnosis of Alzheimer's disease and amnestic mild cognitive impairment: value of magnetic resonance spectroscopy, perfusion, and diffusion tensor imaging of the posterior cingulate region. J Alzheimers Dis. 2011;27(3):591–601.
41. Lim TS, et al. Functional investigation of bilateral posterior cingulate gyri using multivoxel MR spectroscopy. Eur Neurol. 2012;67(5):279–86.
42. Lim TS, et al. Metabolite investigation in both anterior and posterior cingulate gyri in Alzheimer's disease spectrum using 3-tesla MR spectroscopy. Dement Geriatr Cogn Disord. 2012;33(2–3):149–55.
43. Shiino A, et al. The profile of hippocampal metabolites differs between Alzheimer's disease and subcortical ischemic vascular dementia, as measured by proton magnetic resonance spectroscopy. J Cereb Blood Flow Metab. 2012;32(5):805–15.
44. Wang T, et al. Using proton magnetic resonance spectroscopy to identify mild cognitive impairment. Int Psychogeriatr. 2012;24(1):19–27.
45. Watanabe T, Shiino A, Akiguchi I. Hippocampal metabolites and memory performances in patients with amnestic mild cognitive impairment and Alzheimer's disease. Neurobiol Learn Mem. 2012;97(3):289–93.
46. Fayed N, et al. Higher glutamate+ glutamine and reduction of *N*-acetylaspartate in posterior cingulate according to age range in patients with cognitive impairment and/or pain. Acad Radiol. 2014;21(9):1211–7.
47. Graff-Radford J, et al. Regional proton magnetic resonance spectroscopy patterns in dementia with Lewy bodies. Neurobiol Aging. 2014;35(6):1483–90.
48. Zou JX, et al. 3.0 T MRI arterial spin labeling and magnetic resonance spectroscopy technology in the application of Alzheimer's disease. Exp Gerontol. 2014;60:31–6.
49. Jahng G-H, et al. Glutamine and glutamate complex, as measured by functional magnetic resonance spectroscopy, alters during face-name association task in patients with mild cognitive impairment and Alzheimer's disease. J Alzheimers Dis. 2016;52(1):145–59.
50. Su L, et al. Whole-brain patterns of (1)H-magnetic resonance spectroscopy imaging in Alzheimer's disease and dementia with Lewy bodies. Transl Psychiatry. 2016;6(8): e877.
51. González-Domínguez R, Sayago A, Fernández-Recamales Á. Metabolomics in Alzheimer's disease: the need of complementary analytical platforms for the identification of biomarkers to unravel the underlying pathology. J Chromatogr B. 2017;1071:75–92.
52. Joe E, et al. 1 H MRS spectroscopy in preclinical autosomal dominant Alzheimer disease. Brain Imaging Behav. 2018;13:1–8.
53. Kwo-On-Yuen PF, et al. Brain *N*-acetyl-l-aspartic acid in Alzheimer's disease: a proton magnetic resonance spectroscopy study. Brain Res. 1994;667(2):167–74.
54. Murray ME, et al. Early Alzheimer's disease neuropathology detected by proton MR spectroscopy. J Neurosci. 2014;34(49):16247–55.
55. Mutlu J, et al. Connectivity disruption, atrophy, and hypometabolism within posterior cingulate networks in Alzheimer's disease. Front Neurosci. 2016;10:582.
56. Pardon MC, et al. Magnetic resonance spectroscopy discriminates the response to microglial stimulation of wild type and Alzheimer's disease models. Sci Rep. 2016;6:19880.
57. Waragai M, Moriya M, Nojo T. Decreased *N*-acetyl aspartate/myo-inositol ratio in the posterior cingulate cortex shown by magnetic resonance spectroscopy may be one of the risk markers of preclinical Alzheimer's disease: a 7-year follow-up study. J Alzheimers Dis. 2017;60(4):1411–27.
58. Yeh YC, et al. Association between altered neurochemical metabolites and apathy in patients with Alzheimer's disease. Int Psychogeriatr. 2018;30(5):761–8.
59. Yilmaz A, et al. Diagnostic biomarkers of Alzheimer's disease as identified in saliva using 1H NMR-based metabolomics. J Alzheimers Dis. 2017;58(2):355–9.
60. Schröder J, Pantel J. Neuroimaging of hippocampal atrophy in early recognition of Alzheimer's disease—a critical appraisal after two decades of research. Psychiatry Res Neuroimaging. 2016;247:71–8.
61. Henneman WJ, et al. Hippocampal atrophy rates in Alzheimer disease: added value over whole brain volume measures. Neurology. 2009;72(11):999–1007.
62. Andrews-Hanna JR, et al. Functional-anatomic fractionation of the brain's default network. Neuron. 2010;65(4):550–62.
63. Zhou Y, et al. Abnormal connectivity in the posterior cingulate and hippocampus in early Alzheimer's disease and mild cognitive impairment. Alzheimers Dement. 2008;4(4):265–70.
64. Bai F, et al. Mapping the altered patterns of cerebellar resting-state function in longitudinal amnestic mild cognitive impairment patients. J Alzheimers Dis. 2011;23(1):87–99.
65. Braak H, Braak E. Neuropathological stageing of Alzheimer-related changes. Acta Neuropathol. 1991;82(4):239–59.
66. Battaglia FP, et al. The hippocampus: hub of brain network communication for memory. Trends Cogn Sci. 2011;15(7):310–8.
67. Eichenbaum H. Prefrontal-hippocampal interactions in episodic memory. Nat Rev Neurosci. 2017;18(9):547–58.
68. Baslow MH. The vertebrate brain, evidence of its modular organization and operating system: insights into the brain's basic units of structure, function, and operation and how they influence neuronal signaling and behavior. Front Behav Neurosci. 2011;5:5.
69. Moffett JR, et al. *N*-Acetylaspartate: a unique neuronal molecule in the central nervous system, vol. 576. Boston: Springer; 2006.
70. Strumia E, Pelliccia F, D'Ambrosio G. Creatine phosphate: pharmacological and clinical perspectives. Adv Ther. 2012;29(2):99–123.
71. Bittner DM, Heinze HJ, Kaufmann J. Association of 1H-MR spectroscopy and cerebrospinal fluid biomarkers in Alzheimer's disease: diverging behavior at three different brain regions. J Alzheimers Dis. 2013;36(1):155–63.
72. Tayebati SK, Amenta F. Choline-containing phospholipids: relevance to brain functional pathways. Clin Chem Lab Med. 2013;51(3):513–21.
73. Iorio E, et al. Choline metabolic profiling by magnetic resonance spectroscopy. Methods Mol Biol. 2013;1049:255–70.
74. Bai XC, et al. An atomic structure of human gamma-secretase. Nature. 2015;525(7568):212–7.
75. Teranishi Y, et al. Proton myo-inositol cotransporter is a novel gamma-secretase associated protein that regulates Abeta production without affecting Notch cleavage. FEBS J. 2015;282(17):3438–51.
76. Maragakis NJ, Rothstein JD. Glutamate transporters: animal models to neurologic disease. Neurobiol Dis. 2004;15(3):461–73.
77. Bar-Peled O, et al. Distribution of glutamate transporter subtypes during human brain development. J Neurochem. 1997;69(6):2571–80.
78. Chen HSV, Lipton SA. The chemical biology of clinically tolerated NMDA receptor antagonists. J Neurochem. 2006;97(6):1611–26.

Publisher's Note